

7. R. S. R. Gorla, "Combined natural and forced convection in a laminar wall jet along vertical plate with uniform surface heat flux," Appl. Sci. Res., 31, No. 6 (1976).
8. G. Bateman and A. Erdelyi, Higher Transcendental Functions. Hypergeometric Function. Legendre Function, McGraw-Hill.
9. G. Bateman and A. Erdelyi, Higher Transcendental Functions. Bessel Functions, Parabolic Cylindrical Functions, and Orthogonal Polynomials, McGraw-Hill.
10. B. P. Beloglazov and A. S. Ginevskii, "Computation of laminar satellite jets with exact satisfaction of the condition of constant excess momentum," Uch. Zap. Central Aero-Hydrodynamic Institute (TsAGI), 5, No. 4 (1974).

COLLISION OF PLANE, VISCOUS, MULTILAYERED JETS

M. V. Rubtsov

UDC 532.522+532.526

In order to determine the differences in real flow with high-speed collision of metallic plates from known [1, 2] inviscid flow, Rubtsov [3] considered the problem of symmetric impingement of plane viscous jets with free boundary. The problem is solved approximately assuming boundary-layer corrections to inviscid flow near the free boundaries at sufficiently large Reynolds numbers. A solution is obtained to the first approximation from simplified correction $w(\varphi, \psi)$ to the inviscid velocity $u_0(\varphi, \psi)$ along the stream line. The simplified equation is obtained from Navier-Stokes equations by carrying out order-of-magnitude analysis. It is of interest to use this method to study the problem of jet collision when each jet comprises a number of layers with different viscosity but the same density.

1. Consider stationary inviscid flow in the region shown in Fig. 1. Two jets of equal thickness h flow from infinity with the same velocity U at an angle γ to the axis of symmetry. The x axis is along the axis of symmetry. Consider half the flow region. The free jet consists of N layers of equal density ρ and different viscosity μ_l and thickness δ_l , $l = 1, 2,$

\dots, N , $\sum_{l=1}^N \delta_l = h$. The flow region is limited by the x axis and two free boundaries Σ_1 and

Σ_2 . There are $N - 1$ boundaries in the flow region $\Gamma_1, \Gamma_2, \dots, \Gamma_{N-1}$. The velocity components along x and y are denoted by u and v . Normalizing x and y by h , u, v by U , and pressure p by ρU^2 , Navier-Stokes equations are written in the form

$$\begin{aligned} u_l \frac{\partial u_l}{\partial x} + v_l \frac{\partial u_l}{\partial y} &= - \frac{\partial p_l}{\partial x} + \frac{1}{\text{Re}_l} \Delta u_l, \\ u_l \frac{\partial v_l}{\partial x} + v_l \frac{\partial v_l}{\partial y} &= - \frac{\partial p_l}{\partial y} + \frac{1}{\text{Re}_l} \Delta v_l, \end{aligned} \quad (1.1)$$

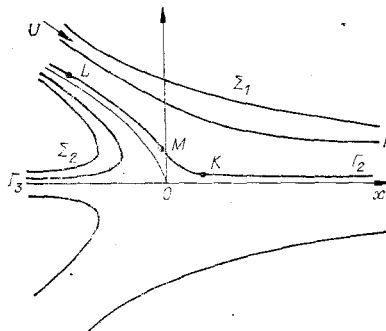


Fig. 1

Novosibirsk. Translated from Zhurnal Prikladnoi Mekhaniki i Tekhnicheskoi Fizika, No. 2, pp. 34-41, March-April, 1984. Original article submitted January 26, 1983.

$$\frac{\partial u_l}{\partial x} + \frac{\partial v_l}{\partial y} = 0, \quad \text{Re}_l = \frac{\rho U h}{\mu_l}, \quad l = 1, 2, \dots, N.$$

Boundary conditions at Σ_1 and Σ_2 are given in [3]:

$$\mathbf{V}|_{\Sigma} \cdot \mathbf{n} = 0, \quad \mathbf{n} \cdot \mathbf{T}|_{\Sigma} \cdot \boldsymbol{\tau} = 0, \quad \mathbf{n} \cdot \mathbf{T}|_{\Sigma} \cdot \mathbf{n} = 0, \quad (1.2)$$

where \mathbf{n} and $\boldsymbol{\tau}$ are unit vectors of the outward normal and tangent to the boundary Σ ; \mathbf{V} is the velocity vector; \mathbf{T} is the stress tensor

$$T_{ij} = -p\delta_{ij} + 2\mu(\partial u_i/\partial x_j + \partial u_j/\partial x_i), \quad i, j, = 1, 2, \\ x_1 = x, \quad x_2 = y, \quad u_1 = u, \quad u_2 = v.$$

Boundary conditions on Γ_l are chosen from continuity conditions for velocity vectors and stresses

$$\mathbf{V}|_{\Gamma} \cdot \mathbf{n} = 0, \quad \mathbf{V}_+|_{\Gamma} \cdot \boldsymbol{\tau} = \mathbf{V}_-|_{\Gamma} \cdot \boldsymbol{\tau}, \\ \mathbf{n} \cdot \mathbf{T}_+|_{\Gamma} \cdot \boldsymbol{\tau} = \mathbf{n} \cdot \mathbf{T}_-|_{\Gamma} \cdot \boldsymbol{\tau}, \quad \mathbf{n} \cdot \mathbf{T}_+|_{\Gamma} \cdot \mathbf{n} = \mathbf{n} \cdot \mathbf{T}_-|_{\Gamma} \cdot \mathbf{n}. \quad (1.3)$$

The problem consists in the determination of functions u_l , v_l , and p_l satisfying conditions (1.1)-(1.3).

2. Assuming that functions u_l , v_l , p_l are sufficiently smooth and as $\min_l \text{Re}_l \rightarrow \infty$ the

basic flow becomes inviscid [1, 2], Eqs. (1.1) are written in orthogonal coordinates (φ, ψ) , where φ and ψ are the real and imaginary parts of the complex potential of the inviscid flow. Dropping the index l ,

$$\frac{u}{H_1} \frac{\partial u}{\partial \varphi} + \frac{g}{H_2} \frac{\partial u}{\partial \psi} + \frac{g}{H_1 H_2} \left(u \frac{\partial H_1}{\partial \psi} - g \frac{\partial H_2}{\partial \varphi} \right) = -\frac{1}{H_1} \frac{\partial p}{\partial \varphi} + \frac{1}{H_2 \text{Re}} \frac{\partial}{\partial \psi} \left\{ \frac{1}{H_1 H_2} \left(\frac{\partial u H_1}{\partial \psi} - \frac{\partial g H_2}{\partial \varphi} \right) \right\}, \quad (2.1)$$

$$\frac{u}{H_1} \frac{\partial g}{\partial \varphi} + \frac{g}{H_2} \frac{\partial g}{\partial \psi} + \frac{u}{H_1 H_2} \left(g \frac{\partial H_2}{\partial \varphi} - u \frac{\partial H_1}{\partial \psi} \right) = -\frac{1}{H_2} \frac{\partial p}{\partial \psi} + \frac{1}{H_1 \text{Re}} \frac{\partial}{\partial \varphi} \left\{ \frac{1}{H_1 H_2} \left(\frac{\partial g H_2}{\partial \varphi} - \frac{\partial u H_1}{\partial \psi} \right) \right\}, \quad \frac{\partial u H_2}{\partial \varphi} + \frac{\partial g H_1}{\partial \psi} = 0.$$

Here u and g in (2.1) denote velocity components along the φ and ψ axes, H_1 and H_2 are Lamé coefficients. If u_0 is the inviscid flow velocity along the streamline, then $H_1 = H_2 = 1/u_0$.

Simplified equations of motion were obtained in [3] with order-of-magnitude analysis. In the present work consider the asymptotic expansion of the solution in powers of ϵ where the small parameter $\epsilon^2 = 1/\text{Re}$ is negligible at large Re [4-6]. The analysis is limited to two-term inner and outer expansions. For the outer expansion,

$$u^0 = u_0 + \epsilon u^1, \quad g^0 = g_0 + \epsilon g^1, \quad p^0 = p_0 + \epsilon p^1, \quad (2.2)$$

where the zeroth approximation u_0 , $g_0 \equiv 0$, and p_0 is the known inviscid potential flow. Substituting (2.2) in (2.1) and equating terms of the same order in ϵ , we get first-order approximation for the outer expansion

$$u_1 \partial u_0 / \partial \varphi + u_0 \partial u^1 / \partial \varphi = -\partial p^1 / \partial \varphi, \\ u_0 \frac{\partial g^1}{\partial \varphi} + 2u^1 \frac{\partial u_0}{\partial \psi} - g^1 \frac{\partial u_0}{\partial \varphi} = -\frac{\partial p^1}{\partial \psi}, \quad \frac{\partial u^1 / u_0}{\partial \varphi} + \frac{\partial g^1 / u_0}{\partial \psi} = 0,$$

whence

$$\frac{\partial u^1 / u_0}{\partial \psi} - \frac{\partial g^1 / u_0}{\partial \varphi} = 0, \quad \frac{\partial u^1 / u_0}{\partial \varphi} + \frac{\partial g^1 / u_0}{\partial \psi} = 0, \quad u_0 u^1 + p^1 = 0, \quad (2.3)$$

i.e., $(u^1 - ig^1)/u_0$ is an analytic function. The third equation in (2.3) is obtained from parallel-flow condition as $\varphi \rightarrow -\infty$ and $p^1(-\infty, \psi) = 0$, $u^1(-\infty, \psi) = 0$.

Matching zeroth (single-term) approximations of the outer and inner expansions leads to $u_i = u_0$, $g_i = 0$, $p_i = p_0$ [5]. Consider two-term inner expansion

$$u_i = u_0 + \epsilon \tilde{w}, \quad g_i = \epsilon g_1 + \epsilon^2 g_2, \quad p_i = p_0 + \epsilon p_1.$$

Writing incompressible continuity equation in inner variables $(\varphi, \tilde{\psi})$

$$\frac{\partial g_1/u_0}{\partial \tilde{\psi}} = 0, \quad \frac{\partial \tilde{w}/u_0}{\partial \varphi} + \frac{\partial g_2/u_0}{\partial \tilde{\psi}} = 0,$$

hence $g_1/u_0 = a(\varphi)$. Since the function g_1/u_0 is a constant inside the boundary layer for $\varphi = \text{const}$, matching the outer expansion g^1 with inner expansion g_1 at the outer boundary of the boundary layer, we get

$$g^1(\varphi, \psi = \psi_0)/u_0(\varphi, \psi = \psi_0) = a(\varphi). \quad (2.4)$$

It follows from (2.4) that the harmonic function is continuous across adjacent layers through a linear boundary layer in variables (φ, ψ) as $\varepsilon \rightarrow 0$. Consequently, the function g^1/u_0 can be analytically continued through inner boundary layers over the entire flow region [7]. In the analytical continuation at each layer the harmonic function, u^1/u_0 is determined to the accuracy of the constant, though it follows from the condition $u^1(\varphi, \psi) \rightarrow 0$, $g^1(\varphi, \psi) \rightarrow 0$ at $\varphi \rightarrow -\infty$ that this constant equals zero.

By writing equations of motion in inner variables it is possible to obtain in the limit $\varepsilon \rightarrow 0$,

$$\frac{\partial \tilde{w}u_0}{\partial \varphi} = -\frac{\partial p_1}{\partial \varphi} + \frac{\partial}{\partial \tilde{\psi}} \left\{ u_0^2 \frac{\partial \tilde{w}/u_0}{\partial \tilde{\psi}} \right\}, \quad \frac{\partial p_1}{\partial \tilde{\psi}} = 0. \quad (2.5)$$

In deriving Eq. (2.5) it was taken into account that $\partial u_0/\partial \tilde{\psi} \rightarrow 0$ as $\varepsilon \rightarrow 0$. It follows from the third boundary condition (1.2), written in the inner variables, that

$$\left[p_0 + \varepsilon p_1 + 2\varepsilon^3 \left(u_0 \frac{\partial \tilde{w}}{\partial \varphi} - g_1 \frac{\partial u_0}{\partial \tilde{\psi}} \right) \right] \Big|_{\Sigma} = 0$$

or

$$p_1|_{\Sigma} = -2\varepsilon^2 \left(u_0 \frac{\partial \tilde{w}}{\partial \varphi} - g_1 \frac{\partial u_0}{\partial \tilde{\psi}} \right) \Big|_{\Sigma} \quad (2.6)$$

and in the limit as $\varepsilon \rightarrow 0$, $p_1|_{\Sigma} = 0$. Since $p_1(\varphi, \tilde{\psi}) \equiv 0$ in the boundary layer at the free boundary, then, matching the outer expansion for pressure $p_0 + \varepsilon p^1$ with inner expansion $p_0 + \varepsilon p_0$, we get, according to Eq. (2.6),

$$p^1|_{\Sigma} = 0. \quad (2.7)$$

Besides, at the outer edge of the boundary layer we have from Eq. (2.3)

$$u_0 u^1|_{\Sigma} + p^1|_{\Sigma} = 0. \quad (2.8)$$

Comparing (2.7) and (2.8), we observe that

$$u^1|_{\Sigma} = 0. \quad (2.9)$$

According to the maxima principle for harmonic function $u^1(\varphi, \psi)/u_0(\varphi, \psi)$, determined in the entire flow region, we have, in view of Eq. (2.9),

$$u^1(\varphi, \psi) \equiv 0. \quad (2.10)$$

For the function $g^1(\varphi, \psi)/u_0(\varphi, \psi)$ conjugate to u^1/u_0 , it is true that

$$g^1(\varphi, \psi)/u_0(\varphi, \psi) \equiv \text{const},$$

and from the condition $g^1(\varphi, \psi) \rightarrow 0$ as $\varphi \rightarrow -\infty$ we have $g^1(\varphi, \psi) \equiv 0$.

Using the third equation in (2.3) and (2.10), it is possible to note that, at the outer boundaries of inner boundary layers $p^1(\varphi) = 0$ and matching the outer and inner expansions for pressure gives $p_1(\varphi, \tilde{\psi}) \equiv 0$. Then the first equation in (2.5) is written in the form

$$\frac{\partial \tilde{w}u_0}{\partial \varphi} = \frac{\partial}{\partial \tilde{\psi}} \left(u_0^2 \frac{\partial \tilde{w}/u_0}{\partial \tilde{\psi}} \right) = \frac{\partial^2 \tilde{w}u_0}{\partial \tilde{\psi}^2}. \quad (2.11)$$

Thus, coefficients of first-order terms in ε in the asymptotic expansion of the solution appear to be zero except \tilde{w} in the inner expansion. Uniformly valid first-order approximation in ε will be

$$u = u_0(\varphi, \psi) + \varepsilon \tilde{w}(\varphi, \tilde{\psi}), \quad g(\varphi, \psi) \equiv 0, \quad p(\varphi, \psi) = p_0(\varphi, \psi).$$

Returning to outer variables, Eq. (2.11) can be written in the form

$$\frac{\partial w u_0}{\partial \varphi} = \varepsilon^2 \frac{\partial^2 w u_0}{\partial \psi^2} = \frac{1}{\text{Re}} \frac{\partial^2 w u_0}{\partial \psi^2}, \quad w = \varepsilon \tilde{w}. \quad (2.12)$$

At the free boundary, $\partial u_0 / \partial \varphi = 0$ and (2.11) takes the form

$$\partial \tilde{w} / \partial \varphi = \partial^2 \tilde{w} / \partial \tilde{\psi}^2,$$

and in the variables (φ, ψ) the equation (2.11) takes the form

$$\frac{\partial w}{\partial \varphi} = \frac{1}{\text{Re}} \frac{\partial^2 w}{\partial \psi^2},$$

obtained in [3] by order-of-magnitude analysis of Navier-Stokes equations. The form of Eq. (2.12) is also convenient because it makes it possible to consider mutual influence of adjacent boundary layers since the distance between boundary layers is finite in outer variables.

Boundary conditions for Eq. (2.12) are

$$\begin{aligned} \left(\frac{\partial u_0^2}{\partial \psi} + \frac{\partial u_0 w}{\partial \psi} \right) \Big|_{\Sigma} &= 0, \quad w_+ |_{\Gamma} = w_- |_{\Gamma}, \\ \frac{1}{\text{Re}_+} \left(\frac{\partial u_0^+}{\partial \psi} + \frac{\partial u_0 w_+}{\partial \psi} \right) \Big|_{\Gamma} &= \frac{1}{\text{Re}_-} \left(\frac{\partial u_0^-}{\partial \psi} + \frac{\partial u_0 w_-}{\partial \psi} \right) \Big|_{\Gamma}. \end{aligned} \quad (2.13)$$

Indices + or - in Eq. (2.13) denote quantities to the right or left of the dividing boundary Γ_l . Using Eq. (2.12) and boundary conditions (2.13), it is possible to find an approximate solution to the present problem which can be found, e.g., numerically.

The characteristic feature of the present problem is that the boundary layers occupy the entire flow downstream at any $\varepsilon \neq 0$. Though the uniform correction w to flow velocity is of the order ε^2 , it is caused by the expansion of boundary layers with correction in w of the order ε . The subsequent terms in the inner expansion introduce relative correction of the order of ε to the computed value of \tilde{w} . It appears reasonable to ignore corrections of the order of ε^2 in the outer expansion since the boundary layers occupy the entire downstream regions.

3. In order to compute the steady-state velocity of diverging jets, integrate the first equation of (2.12) in φ from $-\infty$ to $+\infty$, in ψ from the streamline $\psi = 0$ to the free boundary. We get

$$\begin{aligned} \int_0^{\Sigma} w_{+\infty} u_0 d\psi - \int_0^{\Sigma} w_{-\infty} u_0 d\psi &= -\frac{1}{\text{Re}_k} \int_{-\infty}^{\infty} \frac{\partial u_0 w_k}{\partial \psi} \Big|_{\psi=0} d\varphi + \frac{1}{\text{Re}_k} \int_{-\infty}^{\infty} \frac{\partial u_0 w_k}{\partial \psi} \Big|_{\Gamma_k} d\varphi - \frac{1}{\text{Re}_{k+1}} \int_{-\infty}^{\infty} \frac{\partial u_0 w_{k+1}}{\partial \psi} \Big|_{\Gamma_k} d\varphi + \dots \\ &\dots + \frac{1}{\text{Re}_{N-1}} \int_{-\infty}^{\infty} \frac{\partial u_0 w_{N-1}}{\partial \psi} \Big|_{\Gamma_{N-1}} d\varphi - \frac{1}{\text{Re}_N} \int_{-\infty}^{\infty} \frac{\partial u_0 w_N}{\partial \psi} \Big|_{\Gamma_{N-1}} d\varphi + \frac{1}{\text{Re}_N} \int_{-\infty}^{\infty} \frac{\partial u_0 w_N}{\partial \psi} \Big|_{\Sigma} d\varphi, \end{aligned}$$

Γ_k is the dividing boundary closest to $\psi = 0$. The term $\int_0^{\Sigma} w_{-\infty} u_0 d\psi = 0$ since $w_{-\infty} = 0$ according to the problem, $u_0 \rightarrow 1$ as $\varphi \rightarrow \pm\infty$, therefore, $\int_0^{\Sigma} w_{+\infty} u_0 d\psi = \int_0^{\Sigma} w_{+\infty} d\psi = w_{+\infty} \Delta\psi$ where $\Delta\psi$ is

the jet thickness from the line $\psi = 0$ to the free boundary. The above equation can be rewritten in the following manner using boundary conditions (2.13)

$$w_{+\infty} \Delta\psi = -\frac{1}{\text{Re}_k} \int_{-\infty}^{\infty} \frac{\partial u_0 w_k}{\partial \psi} \Big|_{\psi=0} d\varphi + \sum_{l=k}^{N-1} \left(\frac{1}{\text{Re}_{l+1}} - \frac{1}{\text{Re}_l} \right) \int_{-\infty}^{\infty} \frac{\partial u_0^2}{\partial \psi} \Big|_{\Gamma_l} d\varphi - \frac{1}{\text{Re}_N} \int_{-\infty}^{\infty} \frac{\partial u_0^2}{\partial \psi} \Big|_{\Sigma} d\varphi. \quad (3.1)$$

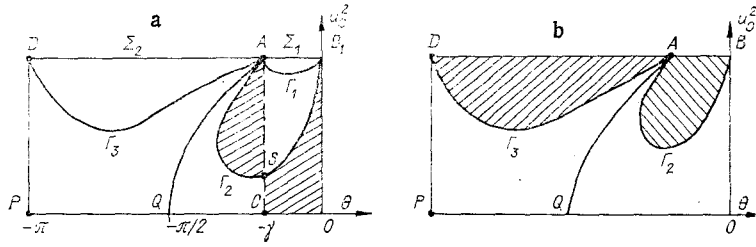


Fig. 2

Consider the expression $\int \frac{\partial u_0^2}{\partial \psi} d\varphi$. The derivative $\partial u_0^2 / \partial \psi$ can be written as $2u_0^2 \partial \ln u_0 /$

$\partial \psi$. For the Zhukovsky function $\ln u_0 - i\theta$ (θ is the argument of the complex velocity) the following Cauchy-Riemann conditions are valid:

$$\partial \ln u_0 / \partial \varphi = -\partial \theta / \partial \psi, \quad \partial \ln u_0 / \partial \psi = \partial \theta / \partial \varphi,$$

hence

$$\partial u_0^2 / \partial \psi = 2u_0^2 \partial \theta / \partial \varphi. \quad (3.2)$$

We will assume that the Reynolds number Re_k of the layer containing the stagnation point is so large that the derivative

$$\left| \frac{\partial u_0 w_k}{\partial \psi} \right|_{\psi=0, \varphi < 0} \ll \left| \frac{\partial u_0 w_k}{\partial \psi} \right|_{\Gamma_k, \varphi < 0},$$

Γ_k is the dividing boundary of the layer containing the stagnation point. When $\varphi > 0$, $\partial u_0 w / \partial \psi |_{\psi=0}$ in view of the flow symmetry. Then the first term on the right-hand side of (3.1) can be neglected. With the help of Eq. (3.2), Eq. (3.1) is written in the form

$$\frac{w_{+\infty} \Lambda \psi}{2} = \sum_{l=k}^{N-1} \left(\frac{1}{Re_{l+1}} - \frac{1}{Re_l} \right) \int_{\psi=\Gamma_l} u_0^2 d\theta - \frac{1}{Re_N} \int_{\psi=\Sigma} d\theta.$$

In the plane (u_0^2, θ) the flow region has the shape of a rectangle OBDP (Fig. 2a). Free boundaries Σ_1 and Σ_2 lie on BD. The point A corresponds to infinity in the free jet, points B and D represent infinity in thick and thin diverging jets. Boundaries Γ_1 , Γ_2 , and Γ_3 are given by lines $A\Gamma_1B$, $A\Gamma_2SB$, and $A\Gamma_3D$. Lines AQ, PD, and OB denote lines $\psi = 0$ and OP represents the stagnation point. When $\psi < \cos \gamma/2$, it is typical for the thick jet to have a two-valued region $A\Gamma_2S$ for the curve $u_0^2(\psi, \theta) |_{\psi=\text{const}}$. The value of the integral $\int u_0^2 d\theta$ for the thick jet when $\psi > \cos \gamma/2$ and for the thin jet is equal to the area of the curvilinear quadrilateral $A\Gamma_1BOC$ and $A\Gamma_3DPC$. For the thick jet, when $\psi < \cos \gamma/2$, $\int u_0^2 d\theta$ is equal to the difference in the shaded areas BSCO and $A\Gamma_2S$. Numerical results of integrating $\int_{\psi=c} u_0^2 d\theta$ for a thick jet are given in the table. ψ_Σ denotes the value of ψ on the free boundary.

In the particular case of two-layered jet

$$\frac{w_{+\infty} \Lambda \psi}{2} = \left(\frac{1}{Re_2} - \frac{1}{Re_1} \right) \int_{\psi=\Gamma} u_0^2 d\theta - \frac{1}{Re_2} \int_{\psi=\Sigma} d\theta. \quad (3.3)$$

If the thin jet is two-layered and $Re_1, Re_2 \neq \infty$, then $\frac{w_{+\infty} \Lambda \psi}{2} = -\frac{(1 - \cos \gamma) w_{+\infty}}{4}$ and $\int_{\psi=\Sigma} d\theta = -(\pi - \gamma)$, whence

$$w_{+\infty} = -\frac{4}{(1 - \cos \gamma)} \left[\frac{\pi - \gamma}{Re_2} + \left(\frac{1}{Re_2} - \frac{1}{Re_1} \right) \int_{\psi=\Gamma} u_0^2 d\theta \right].$$

Analogously for a thick jet,

$$w_{+\infty} = \frac{4}{(1 + \cos \gamma)} \left[-\frac{\gamma}{Re_2} + \left(\frac{1}{Re_2} - \frac{1}{Re_1} \right) \int_{\psi=\Gamma} u_0^2 d\theta \right].$$

TABLE 1

c/ψ_{Σ}	Collision angle		
	45°	60°	75°
0,0025	-0,506	-0,450	-0,387
0,005	-0,442	-0,406	-0,353
0,010	-0,347	-0,335	-0,298
0,015	-0,276	-0,278	-0,253
0,020	-0,220	-0,231	-0,213
0,025	-0,174	-0,190	-0,178
0,030	-0,136	-0,155	-0,147
0,035	-0,103	-0,123	-0,119
0,040	-0,074	-0,095	-0,093
0,045	-0,048	-0,069	-0,069
0,05	-0,026	-0,046	-0,047
0,10	0,112	0,109	0,112
0,20	0,222	0,253	0,279
0,40	0,303	0,375	0,436
0,60	0,342	0,437	0,524
0,80	0,369	0,482	0,592
1,00	0,393	0,524	0,654

When $Re_1 \gg Re_2$ (more viscous outer layer) in the thick jet,

$$w_{+\infty} = -\frac{4}{Re_2(1+\cos\gamma)} \left[\gamma - \int_{\psi=\Gamma} u_0^2 d\theta \right], \quad (3.4)$$

i.e., the quantity w_+ is determined by the area of the curvilinear segments bounded by free boundaries and dividing lines in the plane (u^2_0, θ) (see Fig. 2b). If the inner layer is inviscid ($Re_1 = \infty$) then $w_{+\infty}$ in this layer should be equated to zero. The $w_{+\infty} \Delta\psi = w_{+\infty} \delta$ (δ is the thickness of the viscous layer).

$$w_{+\infty} = -\frac{2}{\delta Re_2} \left[\gamma - \int_{\psi=\Gamma} u_0^2 d\theta \right], \quad (3.5)$$

which differs from (3.4).

The above fact is explained as follows. When $Re_1 \gg Re_2$, it is possible to define two characteristic distances φ_1 and φ_2 from the stagnation point along φ . At the distance φ_1 , $w(\varphi_1)$ is close to Eq. (3.5) in the viscous layer δ and close to zero in the inner layer. At the distance φ_2 the correction $w(\varphi_2)$ is equalized along the diverging jet section and is close to Eq. (3.4). When $Re_1 \rightarrow \infty$, φ_1 and φ_2 increase unboundedly. Hence, in following the distance φ_1 , when $\varphi_1 \rightarrow \infty$, we get the case (3.5) and from the distance φ_2 we get the case (3.4).

When $Re_2 \gg Re_1$ (more viscous inner layer) in the thick jet,

$$w_{+\infty} = -\frac{4}{Re_1(1+\cos\gamma)} \int_{\psi=\Gamma} u_0^2 d\theta. \quad (3.6)$$

An interesting feature of Eq. (3.6) is that when Γ is close to Σ , $\int_{\psi=\Gamma} u_0^2 d\theta$ is positive,

but when $\psi < \psi_*$, where ψ_* is determined only from the impingement angle γ , the integral

$\int_{\psi=\Gamma} u_0^2 d\theta$ changes sign and the correction w to velocity u_0 becomes positive, i.e., the velocity of the thick jet increases after collision. This result is interesting because, in a viscous fluid energy dissipation as a result of internal friction usually results in a reduction in mass rate. In the present case, there is a restructuring of the flow in such a way that the velocity of a thick jet happens to be greater than the inviscid flow in which there is no energy dissipation. Mechanically, an increase in steady-state velocity in the inner layer can be explained by the fact that sufficiently close to $\psi = 0$ lines Γ , the convex region LM (see Fig. 1), where w increases, is much larger than the concave segment MK where w decreases; hence the total increment in w happens to be positive.

Let us determine the increment in mass flow M , momentum J , and kinetic energy E carried away by thick, two-layered jet, in comparison with the inviscid case. Let k_1 and k_2 be the thickness, and let w_1 and w_2 be the uniform corrections to diverging jet velocities. Conservation of mass and momentum along the x axis is written as

$$k_1 U(1 + w_1) + k_2 U(1 + w_2) = 2hU, \quad k_2 U^2(1 + w_2)^2 - k_1 U^2(1 + w_1)^2 = 2hU^2 \cos \gamma.$$

Eliminating k_1 ,

$$k_2 = h(1 + \cos \gamma + w_1(1 - \cos \gamma)/2 - 3(1 + \cos \gamma)w_2/2).$$

It follows from (3.3) that $w_1 < 0$ always. When $w_2 > 0$, $k_2 < k_2^0 = h(1 + \cos \gamma)$, where k_2^0 is the thickness of the thick jet. Expressions for M , J , and E are written in the form

$$\begin{aligned} M &= k_2 U(1 + w_2) = hU \left(1 + \cos \gamma + \frac{w_1(1 - \cos \gamma)}{2} - \frac{w_2(1 + \cos \gamma)}{2} \right) < M_0, \\ J &= k_2 U^2(1 + w_2)^2 = hU^2 \left(1 + \cos \gamma + \frac{w_1(1 - \cos \gamma)}{2} + \frac{w_2(1 + \cos \gamma)}{2} \right) < J_0, \\ E &= \frac{k_2 U^3}{2}(1 + w_2)^3 = \frac{hU^3}{2} \left(1 + \cos \gamma + \frac{w_1(1 - \cos \gamma)}{2} + \frac{3w_2(1 + \cos \gamma)}{2} \right). \end{aligned} \quad (3.7)$$

The index 0 denotes corresponding characteristics of inviscid thick jet. The inequality $M < M_0$ is obvious. Consider the inequality $J < J_0$.

The sum of corrections $w_1(1 - \cos \gamma)/2 + w_2(1 + \cos \gamma)/2$ can be written as

$$s_1 + s_2 = \frac{w_1(1 - \cos \gamma)}{2} + \frac{w_2(1 + \cos \gamma)}{2} = \frac{2}{\text{Re}} \left(\int_{A\Gamma_3 D} u_0^2 d\theta - \int_{A\Gamma_2 B} u_0^2 d\theta \right).$$

The difference in integrals $\int_{A\Gamma_3 D} u_0^2 d\theta$ and $\int_{A\Gamma_2 B} u_0^2 d\theta$ is equal to the unshaded area in Fig. 2b, with a negative sign; hence $s_1 + s_2 < 0$ and $J < J_0$. The increment in kinetic energy flux is determined as the sum

$$s_1 + 3s_2 = \frac{2}{\text{Re}} \left(\int_{A\Gamma_3 D} u_0^2 d\theta - \int_{A\Gamma_2 B} u_0^2 d\theta - 2 \int_{A\Gamma_2 B} u_0^2 d\theta \right),$$

from which it is seen that there are possible flow situations (thick and thin jets should be two-layered with sufficiently thin inner viscous layer), when the kinetic energy flux E carried by the thick jet will be greater than the corresponding flux in the inviscid case. Actually, the unshaded area in Fig. 2b decreases without any limit as Γ_2 and Γ_3 approach $\psi =$

0 and $\int_{A\Gamma_2 B} u_0^2 d\theta$ approaches the area of the curvilinear triangle AQC (see Fig. 2a), i.e., ap-

proaches a finite value. Expressions for mass flux m , momentum j , and energy e for the thin jet are written in the form

$$\begin{aligned} m &= k_1 U(1 + w_1) = hU \left[1 - \cos \gamma + \frac{w_2(1 + \cos \gamma)}{2} - \frac{w_1(1 - \cos \gamma)}{2} \right], \\ j &= k_1 U^2(1 + w_1)^2 = hU^2 \left[1 - \cos \gamma + \frac{w_2(1 + \cos \gamma)}{2} + \frac{w_1(1 - \cos \gamma)}{2} \right], \\ e &= \frac{k_1 U^3}{2}(1 + w_1)^3 = \frac{hU^3}{2} \left[1 - \cos \gamma + \frac{w_2(1 + \cos \gamma)}{2} + \frac{3w_1(1 - \cos \gamma)}{2} \right]. \end{aligned} \quad (3.8)$$

comparing Eqs. (3.7) and (3.8), it is possible to note that $m > m_0$, $j < j_0$, and $e < e_0$, where m_0 , j_0 , and e_0 are the characteristics of the thin jet in the inviscid case. Addition of E from (3.7) and e from (3.8) leads to

$$E + e = E_0 + e_0 + hU^3 [w_2(1 + \cos \gamma) + w_1(1 - \cos \gamma)] = hU^3 [1 + 2(s_1 + s_2)],$$

whence

$$E + e < E_0 + e_0,$$

i.e., the total kinetic energy carried out by both the diverging jets is less than that brought in by the approaching jets by a value that is proportional to the unshaded area in Fig. 2b.

The author acknowledges V. M. Menshchikov for useful suggestions during discussion of the problem.

LITERATURE CITED

1. M. A. Lavrent'ev, "Cumulative charge and its operation," *Usp. Mat. Nauk*, 12, No. 4 (76) (1957).
2. G. Birkhoff, D. McDougall, E. Pugh, and G. Taylor, "Explosives with lined cavities," *J. Appl. Phys.*, 19, 563 (1948).
3. M. V. Rubtsov, "Boundary layer in intersecting plane jets with small viscosity," in: *Dynamics of Continuous Media [in Russian]*, No. 51, Hydrodynamics Institute, Siberian Branch, Academy of Sciences of the USSR, Novosibirsk (1981).
4. M. I. Vishik and L. A. Lyusternik, "Regular singularity and boundary layer for linear differential equations with a small parameter," *Usp. Mat. Nauk*, 12, No. 5(77) (1957).
5. J. D. Cole, *Perturbation Methods in Applied Mathematics*, Parabolic Press (1968).
6. M. Van Dyke, *Perturbation Methods in Fluid Mechanics*, Parabolic Press (1964).
7. M. A. Lavrent'ev and B. V. Shabat, *Methods in Theory of Functions in Complex Variables [in Russian]*, Nauka, Moscow (1973).

COMPARISON OF ONE-DIMENSIONAL MODELS OF FLOWS IN BRANCHED CHANNELS WITH EXPERIMENTAL DATA

S. V. Pavlov and I. K. Yaushev

UDC 533.6.011

One-dimensional modeling is presently the most popular approach to the description of gasdynamic flows in complicated systems containing a large number of tubes or channels coupled with each other. The so-called problem of the decay of an arbitrary discontinuity at a junction acquires an important role in the investigation of the general properties of generalized solutions of one-dimensional equations of gasdynamics in branched systems of channels. This problem has been investigated theoretically in sufficient completeness in a number of reports for the cases of couplings of two and three channels (jumps in cross section [1, 2], local resistance [3], a perforated barrier [4], branched channels with parallel axes [5, 6], and an arbitrary tee [7, 8]), and various self-similar solutions have been constructed. To obtain a complete picture, however, theoretical results must be compared with experimental data, which has been done so far only for certain particular cases of local resistances in two coupled channels. In the present work such a comparison is made for a plane tee formed by the main channel and a side opening of the same width.

We consider one particular case of the decay of a discontinuity, when a shock wave travels through quiescent gas to the branching section. Experiments of this type have been described sufficiently widely in the literature. As a result of the decay of the initial shock front a rarefaction wave is reflected in the main channel 1, while in the straight (channel 2) and side (channel 3) branches shock waves travel, behind which contact discontinuities follow. The self-similar flow pattern obtained in the one-dimensional model for this typical configuration is shown in the form of an x, t wave diagram in Fig. 1, where $x < 0$ corresponds to the main channel at the entrance to the tee, while $x > 0$ corresponds to one of the branches at the exit from the tee, R_1 is the reflected centered rarefaction wave, S_2 and

Novosibirsk. Translated from *Zhurnal Prikladnoi Mekhaniki i Tekhnicheskoi Fiziki*, No. 2, pp. 42-44, March-April, 1984. Original article submitted January 12, 1983.